

MoMEMta, a modular toolkit for the Matrix Element Method at the LHC



Sébastien Brochet, Christophe Delaere, Brieuc François, Vincent Lemaître, Alexandre Mertens, Alessia Saggio, Miguel Vidal Marono, and Sébastien Wertz

*Centre for Cosmology, Particle Physics and Phenomenology (CP3),
Université catholique de Louvain, Chemin du Cyclotron 2, B-1348 Louvain-la-Neuve, Belgium*

ABSTRACT: The Matrix Element Method has proven to be a powerful method to optimally exploit the information available in detector data. Its widespread use is nevertheless impeded by its complexity and the associated computing time. MoMEMta, a C++ software package to compute the integrals at the core of the method, provides a versatile implementation of the Matrix Element Method to both the theory and experiment communities. Its modular structure covers the needs of experimental analysis workflows at the LHC without compromising ease of use on simpler and smaller simulated samples used for phenomenological studies. In this paper, we present version 1.0 of MoMEMta, together with examples illustrating the wide range of application at the LHC accessible for the first time with a single tool.

KEYWORDS: Analysis and statistical methods

ARXIV EPRINT: [1805.08555](https://arxiv.org/abs/1805.08555)

Contents

1	Introduction	1
2	The matrix element method	2
3	Implementation	4
4	MEM use cases	6
4.1	Discovery and characterisation of the Higgs boson	6
4.2	Charge identification in tW production	7
4.3	$t\bar{t}H$ production	9
5	Indicative performance figures	10
6	Summary	11
7	Acknowledgments	12

1 Introduction

The discovery of the Higgs boson by the ATLAS and CMS experiments in 2012 [1, 2] opened a new era in particle physics. More than just a new particle, a new set of interactions needs to be characterised. The LHC physics program therefore includes precision measurements of standard model (SM) processes (in particular in the top and scalar sectors) and the search for rare production mechanisms or rare decay channels. The absence so far of any obvious sign of physics beyond the standard model further increases the need to look in places where the backgrounds are large and the effect of new physics subtle.

In all these studies, it is of the uttermost importance to fully exploit the potential of the large data set collected. For most of the analyses performed in high energy physics (HEP), obtaining an optimal result implies the treatment of multiple correlated quantities in a multivariate setting. The most popular methods for multivariate analysis in HEP are machine learning techniques, such as boosted decision trees and neural networks. These approaches require large training data sets (usually obtained by Monte Carlo techniques) in order to learn the internal structure of the data. On the contrary, the Matrix Element Method (MEM) uses directly our theoretical knowledge of a process to assign to each event a probability that measures the compatibility of experimental data with a given hypothesis. There is no training, since the underlying Lagrangian, from which the matrix element of the partonic process is derived, is known.

The MEM, originally designed at the Tevatron experiments $D\bar{0}$ and CDF [3–10] for top quark mass measurements in $t\bar{t}$ production, is nowadays a common technique in particle physics. Recent examples of its use at the LHC are searches for $t\bar{t}H$ [11–18] and single top quark production [19],

and a measurement of spin correlations in $t\bar{t}$ production [20]. Nevertheless, while it can be used for a wide variety of studies, the practical application of the MEM has been impeded by its complexity and by the associated computing time. In order to evaluate the probability under a given theoretical hypothesis of a given experimental event, a difficult convolution of the theoretical information on the hard scattering (i.e. the matrix element squared) with the experimentally available information on the final state (encoded in the so-called transfer functions) has to be performed. The corresponding integrand varies by several orders of magnitudes in different regions of the phase space, which implies the use of adaptive numerical integration techniques together with a smart choice of integration variables. A general algorithm has been proposed in Ref. [21], which involves optimised phase-space mappings designed to remove as much as possible the peaks in the integrand. However, the corresponding implementation (MADWEIGHT) is not supported anymore and suffers from a lack of flexibility that prevents—or significantly limits—its use in large scale analyses of LHC data by the collaborations. Furthermore, the tool is very rigid and does not allow the user to implement simplifying assumptions

In this paper, we present MoMEMta, a modular C++ software package to compute the convolution integrals at the core of the method. Its modular structure covers the needs of experimental analysis workflows at the LHC without compromising the ease of use on simpler and smaller simulated samples used for phenomenological studies. It relies on the same approach as MADWEIGHT to address the parameterisation of the phase space but leaves more freedom to the user. MoMEMta is designed to be fast, to adapt to any process, and to be integrated in any C++ or Python analysis workflow.

In the following, we will first review the MEM, with an emphasis on the assumptions made in MoMEMta, before presenting shortly the philosophy of the implementation. We will then concentrate on a few concrete use cases that illustrate the variety of problems that can be tackled using MoMEMta, and how the modularity can best be exploited to adapt to these problems.

2 The matrix element method

The MEM is a technique to calculate the conditional probability density $P(x|\alpha)$ to observe an experimental event x , given a specific theoretical hypothesis α . Details about the method can be found for example in Ref. [22]. We will here concentrate on the main aspects.

The likelihood for a partonic final state y to be produced in the hard-scattering process is proportional to the differential cross section $d\sigma_\alpha$ of the corresponding process, given by

$$d\sigma_\alpha(q_1, q_2, y) = \frac{(2\pi)^4 |\mathcal{M}_\alpha(q_1, q_2, y)|^2}{q_1 q_2 s} d\Phi(y), \quad (2.1)$$

where q_1 and q_2 stand for the initial state parton momentum fractions, s stands for the hadronic centre-of-mass energy and y stands for the kinematics of the final state.

The central element in that expression is the squared matrix element for process α , denoted $|\mathcal{M}_\alpha(q_1, q_2, y)|^2$, where the summation over spin and colour states is understood. It can be obtained either analytically or numerically through packages like MG5_AMC@NLO [23] or MCFM [24]. Because of the intrinsic theoretical difficulty to identify final state particles with partons at NLO,

the leading order matrix element is used in most applications. The n-body phase space $d\Phi(y)$ must also be considered in the calculation, as it plays an important role in any change of variable needed for the integration of the differential cross section.

To obtain the differential cross section $d\sigma_\alpha(y)$ in hadron collisions, (2.1) is convoluted with the parton density functions (PDF) and summed over all possible flavour compositions of the colliding partons,

$$d\sigma_\alpha(y) = \int_{q_1, q_2} \sum_{a_1, a_2} dq_1 dq_2 f_{a_1}(q_1) f_{a_2}(q_2) d\sigma_\alpha(q_1, q_2, y), \quad (2.2)$$

where $f_{a_1}(q_1)$ and $f_{a_2}(q_2)$ are the parton density functions for a given flavour a_i and momentum fraction q_i .

The evolution of the parton-level configuration y into a reconstructed event x in the detector is modeled by a transfer function $T(x|y)$, normalised as a probability density over x , that describes how the partonic final state y is reconstructed as x in the detector. This includes the effects from the parton shower, hadronisation, and the limited detector resolution. The efficiency $\epsilon(y)$, i.e. the probability to reconstruct and select a specific partonic configuration y , also needs to be taken into account. This includes geometrical acceptance effects.

The transfer function and efficiency are assumed to factorise into contributions from each measured final-state particle, and each of these contributions are often assumed to further factorise into simple direction- and momentum-dependent terms. For most applications, it is realistic to then assume that the direction is perfectly reconstructed. The transfer function in that case is a Dirac delta function on the angular variables, and takes a non-trivial form only for the energy (or transverse momentum) degree of freedom. All these assumptions may not be valid in cases where objects, especially jets, are close to each other or reconstructed together like in boosted topologies, and will then result in a less accurate result.

Neutrinos (or other invisible particles) cannot be measured directly, but the corresponding volume of phase space over which to integrate can be narrowed by exploiting mass constraints from intermediate resonances assumed to be on-shell, or by relying on momentum conservation in the transverse plane, which yields an estimate of the total transverse momentum \vec{p}_T^{miss} of the missing particles in the event. However, it is not possible to trivially factorise the transfer function on the two components of \vec{p}_T^{miss} from the terms relative to visible particles in the final state, since the experimental error in measuring \vec{p}_T^{miss} is correlated with the error made in measuring all the other particles in the event.

Aspects to be considered in the transfer function and efficiency are the measurement of the momentum of a particle as well as its (mis-)identification. This latter point might be relevant for b quarks and τ leptons, and allows in principle to combine different final states for the same partonic event.

After convolution, the full expression reads

$$P(x|\alpha) = \frac{1}{\sigma_\alpha^{\text{vis}}} \int d\sigma_\alpha(y) T(x|y) \epsilon(y) \quad (2.3a)$$

$$= \frac{1}{\sigma_\alpha^{\text{vis}}} \int \sum_{q_1, q_2} \int_{a_1, a_2} \int_y d\Phi(y) dq_1 dq_2 f_{a_1}(q_1) f_{a_2}(q_2) |\mathcal{M}_\alpha(q_1, q_2, y)|^2 T(x|y) \epsilon(y), \quad (2.3b)$$

where $\sigma_\alpha^{\text{vis}}$ is a normalisation factor that ensures $P(x|\alpha)$ is a probability density over x . Finally, one has also to take into account the fact that some of the particles measured in the detector cannot be assigned unambiguously to specific final-state partons. All possible combinations must be considered and their contributions averaged.

The information contained in (2.3b) can be exploited in different ways, from the extraction of the most probable value of the theory parameters through a likelihood maximisation method [25], for which the normalisation constant $\sigma_\alpha^{\text{vis}}$ has to be properly taken into account, to the bare use of the integral result without normalisation $\sigma_\alpha^{\text{vis}}$, referred to in the literature as matrix element weight, $W(x|\alpha)$.

The integral defined in (2.3b) is typically a small number that varies over several orders of magnitudes from event to event. It is therefore common to use instead the *event information* defined by $I_\alpha \equiv -\log P(x|\alpha)$. When computed from the weight instead of the probability, the information is only modified by an additive constant, with no consequence in many applications. We will denote this quantity $I'_\alpha \equiv -\log W(x|\alpha)$.

In the limit where all the quantities and functions in (2.3b) are known with perfect accuracy, $P(x|\alpha)$ is a likelihood. By the Neyman–Pearson lemma, the ratio between the likelihoods obtained under two different hypotheses α and α' is the most powerful test statistic to discriminate one from the other [26]. Hence, if it can be implemented, the MEM should provide optimal experimental sensitivity. In practice, we are limited by the use of leading-order matrix elements, or by assumptions made in constructing the transfer function. The quantity (2.3b) is therefore not a true likelihood, and the Neyman–Pearson lemma does not strictly apply. For discrimination purposes, it is then common to use the event information as input of another multivariate method (typically a boosted decision tree or a neural network).

3 Implementation

The MEM is used in HEP by both theoretical and experimental communities with different purposes and levels of complexity ranging from the evaluation of a matrix element on a reconstructed event—which does not require any integration process—to the precise evaluation of model parameters (e.g. the top quark mass) through the use of the properly normalised likelihood derived from (2.3b).

In order to adapt to these very different use cases, a modular design has been adopted for MoMEMta. The core library is written in C++ and provides modules for various purposes: to represent and evaluate the matrix element and parton density functions, to represent and evaluate transfer functions, to perform changes of variables, to handle the combinatorics of the final state, etc. That way, every term of (2.3b) is treated as a module that can be configured by the user. Weights are computed for a given process by calling and linking the proper set of modules in a configuration

file written in the Lua scripting language [27]. The resulting object can be called from any C++ or Python code, which means that it seamlessly integrates into the complex analysis environment of the large experimental collaborations but can also be used within small programs reading events from files in any format (e.g. a custom text file, or a file in the ROOT [28], HEPMC [29], LHCO [30] or STDHEP [31] format).

The computation of the weights requires, in most cases, the evaluation of multidimensional integrals via adaptive Monte Carlo techniques. The efficiency in computing these integrals depends on the parameterisation of the phase-space measure used in the integration. In order to map in an efficient way all the structures in the integrand, MoMEMta follows the philosophy introduced by MADWEIGHT [21]. In this approach, a standard parameterisation of the phase-space measure is optimised by using a finite number of *analytic* transformations over subsets of the integration variables, called “blocks”. A list of the blocks available in MoMEMta along with the addressed event topologies, and the integration variables removed and introduced by the changes of variables, is shown in Tabs. 1 and 2. The first table lists “Main Blocks”, i.e. changes of variables that allow to integrate out the four-dimensional Dirac delta function present in the phase-space density term $d\Phi(y)$, that enforces conservation of momentum between the initial and final states. The second table lists “Secondary Blocks”, i.e. simple changes of variables that do not remove any degree of freedom. Main and secondary blocks are implemented as dedicated MoMEMta modules, which can be chained to perform the change of integration variables that is best suited for the problem at hand. Examples are given in Sec. 4.

Table 1. Set of MoMEMta Main Blocks. Each block performs a specific change of integration variables, and removes four degrees of freedom by enforcing momentum conservation between the initial and final states. The third and fourth columns show the integration variables respectively removed and introduced in each block definition. Block G is introduced in this work, in addition to those originally defined in MADWEIGHT. We denote by q_i the Bjorken fractions of the initial-state partons, and by p_i the 4-momentum of a final-state particle, parameterised in polar coordinates by $|p_i|$, θ_i and ϕ_i . Furthermore, we set $s_{i\dots j} = (p_i + \dots + p_j)^2$. In block E, y denotes the rapidity of the total partonic system. Removing a particle, p_i , means removing all three degrees of freedom associated with that particle. Variables that are not explicitly mentioned are understood to remain present as in the standard phase-space parameterisation.

Main block	Topology	Removes	Integrates over
A	$(q_1, q_2) \rightarrow p_1 + p_2$	$q_1, q_2, p_1 , p_2 $	$\theta_1, \phi_1, \theta_2, \phi_2$
B	$(q_1, q_2) \rightarrow s_{12}(\rightarrow p_1 + p_2)$	q_1, q_2, p_1	s_{12}
C	$(q_1, q_2) \rightarrow s_{123} \rightarrow p_3 + s_{12}(\rightarrow p_1 + p_2)$	$q_1, q_2, p_1, p_3 $	$s_{12}, s_{123}, \theta_3, \phi_3$
D	$(q_1, q_2) \rightarrow s_{134}(\rightarrow p_4 + s_{13}(\rightarrow p_1 + p_3)) + s_{256}(\rightarrow p_6 + s_{25}(\rightarrow p_2 + p_5))$	q_1, q_2, p_1, p_2	$s_{13}, s_{134}, s_{25}, s_{256}$
E	$(q_1, q_2) \rightarrow (s_{1234}, y) \rightarrow s_{13}(\rightarrow p_1 + p_3) + s_{24}(\rightarrow p_2 + p_4)$	q_1, q_2, p_1, p_2	$s_{1234}, y, s_{13}, s_{24}$
F	$(q_1, q_2) \rightarrow s_{13}(\rightarrow p_1 + p_3) + s_{24}(\rightarrow p_2 + p_4)$	p_1, p_2	q_1, q_2, s_{13}, s_{24}
G	$(q_1, q_2) \rightarrow s_{12}(\rightarrow p_1 + p_2) + s_{34}(\rightarrow p_3 + p_4)$	$ p_1 , p_2 , p_3 , p_4 $	s_{12}, s_{34}

MoMEMta ships with matrix elements for a few processes, but any leading-order process handled by MG5_AMC@NLO [23] can be added using a Matrix Element Exporter plugin pro-

Table 2. Set of MoMEMta Secondary Blocks. Each block performs a specific change of integration variables, acting exclusively on final-state particles. The third and fourth columns show the integration variables respectively removed and introduced by each change of variables.

Secondary block	Topology	Removes	Integrates over
A	$s_{1234} \rightarrow (s_{123} \rightarrow s_{12}(\rightarrow p_1 + p_2) + p_3) + p_4$	p_1	$s_{1234}, s_{123}, s_{12}$
B	$s_{123} \rightarrow s_{12}(\rightarrow p_1 + p_2) + p_3$	$ p_1 , \theta_1$	s_{12}, s_{123}, ϕ_1
C/D	$s_{12} \rightarrow p_1 + p_2$	$ p_1 $	s_{12}, ϕ_1, θ_1
E	$s_{123} \rightarrow s_{12}(\rightarrow p_1 + p_2) + p_3$	$ p_1 , p_2 $	s_{12}, s_{123}, ϕ_1 $\theta_1, \phi_2, \theta_2$

vided [32]. Native support for other matrix element generators is planned for future releases, but the modular structure already enables the user to wrap any C++ code that computes a matrix element to be used with MoMEMta.

Parton density functions are obtained from LHAPDF6 [33] and the integration is done using the CUBA library [34], that offers a choice of four independent routines for multidimensional numerical integration: Vegas [35], Suave [34], Divonne [36], and Cuhre [37, 38].

The MoMEMta implementation [39] is publicly available, is licensed under the GPLv3, and comes together with an online documentation [40] and tutorials [41].

4 MEM use cases

Nowadays, applications of the MEM in high-energy physics are most often restricted to computing weights $W(x|\alpha)$ under several hypotheses, to discriminate a signal from one or several backgrounds. In complex situations with several reconstructed objects and unconstrained degrees of freedom, there is no unique solution to the problem of efficiently and precisely computing $W(x|\alpha)$, and the user has to play an active role in defining how to evaluate $W(x|\alpha)$ and at which accuracy.

In this section we describe a few use cases of the MEM for signal extraction in LHC analyses. The examples illustrate various levels of complexity, from the simplest case with a precisely reconstructed final state for which no integration is needed, to complex final states including six reconstructed and two unobserved objects. The Lua configuration for each of the examples can be found together with the MoMEMta tutorials [41]. In all the cases simulated events are generated using MG5_AMC@NLO [23], PYTHIA [42] and DELPHES [43].

The computation times vary by several orders of magnitude among the different use cases, and strongly depend on the choice of parameters governing the integration procedure. Indicative performance figures are given in Sec. 5.

4.1 Discovery and characterisation of the Higgs boson

The MEM was instrumental for the CMS collaboration in the discovery of the Higgs boson in the $H \rightarrow ZZ^* \rightarrow 4l$ channel [2]. Likewise, the characterisation by ATLAS [44, 45] and CMS [46, 47] of the discovered resonance in terms of coupling structure, spin and parity, has relied on matrix-element techniques as suggested in Refs. [48, 49]. In this channel, all final-state particles can be detected

and there are no unobserved degrees of freedom to integrate over. Given the good experimental resolution on muon and electron direction and momentum, it is reasonable to approximate the transfer function in (2.3b) by $T(x, y) = \delta(x - y)$. Hence, the integral reduces to a simple evaluation of the matrix element squared and the PDFs using the measured momenta in the event. In this framework, dubbed matrix element likelihood analysis (MELA), it is straightforward to build a discriminating variable between the signal and the $q\bar{q} \rightarrow ZZ \rightarrow 4l$ background by considering the matrix elements of these two hypotheses:

$$\mathcal{D}_{\text{bkg}}(x) = \left(1 + \frac{P(x|\text{bkg})}{P(x|\text{sig})}\right)^{-1}. \quad (4.1)$$

Similar variables can be constructed to discriminate, for instance, a SM Higgs boson ($J^P = 0^+$) from a resonance of the same mass but different spin and/or opposite parity:

$$\mathcal{D}_{J^\pm}(x) = \left(1 + \frac{P(x|J^\pm)}{P(x|0^+)}\right)^{-1}. \quad (4.2)$$

Although MoMEMta was designed to handle more complex final states, its flexibility allows the user to easily implement a MELA-like analysis. To illustrate this fact, we have simulated events for the $gg \rightarrow H \rightarrow ZZ^* \rightarrow 4\mu$ and $q\bar{q} \rightarrow ZZ^*/Z\gamma^* \rightarrow 4\mu$ processes. The SM Higgs sample, as well as the production and decay of a resonance of spin/parity $J^P = 0^-$ were generated using the Higgs characterisation framework [50]. With MoMEMta's plugin for MG5_AMC@NLO, the same matrix elements used for event generation can be exported in a format suitable for MoMEMta. The configuration of MoMEMta in this use case only requires a single module, which returns the product of the matrix element and the PDFs evaluated on a given event. The phase-space density term present in (2.3b) does not need to be included, since it cancels in the ratios in (4.1) and (4.2). With $P(x|\text{bkg})$, $P(x|\text{sig})$ and $P(x|0^-)$ computed by MoMEMta, the discriminant variables \mathcal{D}_{bkg} and \mathcal{D}_{0^-} can be built. The normalised distributions of these variables, for the different processes considered, are shown on Fig. 1 after an event selection closely following the analysis in Ref. [47]. The discrimination power between the concurrent hypotheses is comparable to what is obtained in Refs. [46, 47].

4.2 Charge identification in tW production

The MEM has been extensively used in the study of single top quark production processes at the Tevatron [51, 52], and was instrumental in the most sensitive search for s -channel single top production at the LHC [19]. Incidentally, single top and W boson associated production (tW) provides a good opportunity to showcase MoMEMta's abilities. This process features three propagators in the matrix element and, in the case where both the top and W decay leptonically (dilepton channel), missing information due to the presence of two neutrinos in the final state.

We consider the charge-conjugate processes, tW^- and $\bar{t}W^+$, which yield the same visible final state and have practically the same rate at the LHC. It has been suggested to measure the CKM matrix element $|V_{td}|$ at the LHC using the charge asymmetry between these two processes [53]. This requires the ability to efficiently disentangle them, a task made difficult by the system not being entirely reconstructible in the dilepton channel.

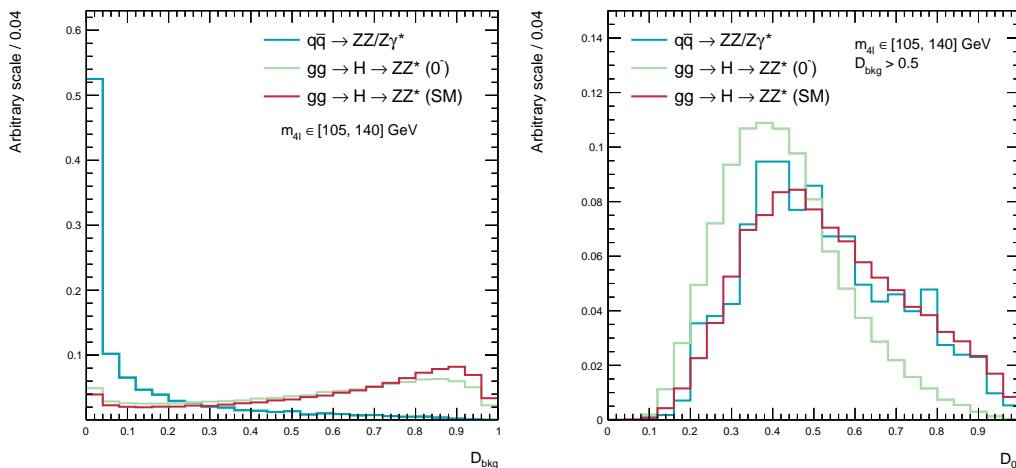


Figure 1. Normalised distribution of the \mathcal{D}_{bkg} (left) and \mathcal{D}_{0^-} (right) variables for the $gg \rightarrow H \rightarrow ZZ^* \rightarrow 4\mu$ and $q\bar{q} \rightarrow ZZ/Z\gamma^* \rightarrow 4\mu$ processes, where the resonance H is taken to be the SM Higgs or a pseudo-scalar of the same mass (0^-). For the right-hand figure, we require $\mathcal{D}_{\text{bkg}} > 0.5$.

We thus suggest to construct a MEM-based observable as:

$$\mathcal{D}_{\pm}(x) = \frac{W(x|\bar{t}W^+) - W(x|tW^-)}{W(x|\bar{t}W^+) + W(x|tW^-)}. \quad (4.3)$$

The charge asymmetry can then be defined by counting the number of events for which either $\mathcal{D}_{\pm}(x) < 0$ or $\mathcal{D}_{\pm}(x) > 0$.

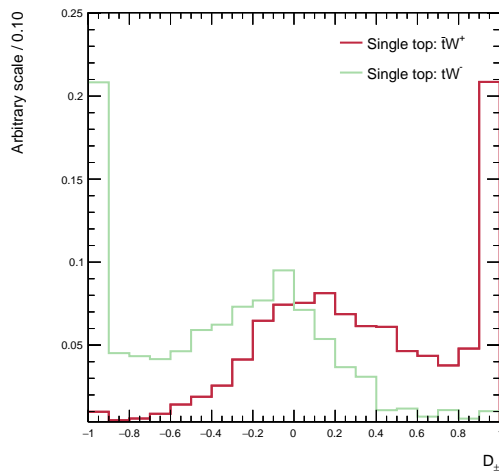


Figure 2. Normalised distribution of the \mathcal{D}_{\pm} asymmetry observable, as defined in (4.3), for the charge-conjugate processes tW^- and $\bar{t}W^+$. Backgrounds such as $t\bar{t}$ production are expected to be distributed symmetrically around zero.

The implementation of the computation of the weights $W(x|\bar{t}W^+)$ and $W(x|tW^-)$ is straightforward in MoMEMta. The directions of all “visible” objects (b quark, leptons) are assumed to

be perfectly reconstructed, and the transfer function reduces to factorised parameterisations of the resolution of their energies. We choose as integration variables the invariant masses of the top quark and both W boson propagators, the energy of the b quark and of the two charged leptons, and the azimuthal direction of the neutrino from the W boson that does not originate from the decay of a top quark (denoted W'). This can be achieved in MoMEMta by pairing the “Secondary Block B” with the “Main Block B”, to handle the phase-space pertaining to the $t \rightarrow b(W \rightarrow \ell\nu)$ and $W' \rightarrow \ell'\nu'$ decay chains, respectively. In addition, the enhancements in the matrix elements due to the top and W propagators can be removed by a further transformation applied on their invariant masses.

The distribution of the \mathcal{D}_\pm discriminant is shown on Fig. 2. About 75% of events from either process can be retained on each side of $\mathcal{D}_\pm = 0$, which by symmetry leads to a corresponding mistag rate of 25%. Depending on the analysis needs, the purity can be further improved at the cost of efficiency (e.g. we obtain 1.5% mistag rate for 25% efficiency).

4.3 $t\bar{t}H$ production

One of the most successful uses of the MEM at the LHC can be found in the searches for $t\bar{t}H$ production. The CMS and ATLAS collaborations have applied the MEM in final states with $H \rightarrow b\bar{b}$ [11–15], and multi-lepton final states with either $H \rightarrow VV$, where $V = W$ or Z , or $H \rightarrow \tau\tau$ [16–18].

Here we demonstrate MoMEMta’s ability to efficiently handle processes as complex as $t\bar{t}H$, featuring a large final-state multiplicity, several propagator enhancements in the matrix element, missing information due to neutrinos, and many possible jet-parton assignments. We consider the channel where the Higgs decays to $b\bar{b}$ and both top quarks decay leptonically, for which the main irreducible background consists of $t\bar{t} + b\bar{b}$ associated production. The relevance of the MEM in this channel was first demonstrated in Ref. [54]. We generate samples for signal and background processes and select events with 2 opposite-charge leptons and at least 4 b-tagged jets.

Weights are computed with MoMEMta under two hypotheses, $t\bar{t}H(b\bar{b})$ and $t\bar{t}b\bar{b}$, using the following parameterisations of the phase-space. The assumptions related to the transfer function are the same as those considered in Sec. 4.2, with the exception of the charged leptons, assumed to be perfectly reconstructed. For both hypotheses, the energies of the b quarks coming from the decays of the top quarks are retained as integration variables. To reduce the number of dimensions to integrate over, we work in the narrow-width approximation (NWA), by which the W boson or top quark propagators are approximated by Dirac delta functions. The momenta of the unobserved neutrinos are then fixed by the constraints on the top quark and W boson invariant masses, as well as by the observed transverse missing momentum in the event. This choice can be implemented by applying the change of variable “Block D” on the standard phase-space parameterisation for the decay products of the top quarks, and fixing the invariants associated with the top quark and W boson propagators (s_{134} , s_{256} , s_{13} and s_{25} in Tab. 1) to their respective pole masses. The remaining degrees of freedom are handled differently, depending on the hypothesis:

- $t\bar{t}b\bar{b}$: The standard polar phase-space parameterisation for the two extra b quarks is retained, i.e. we integrate over both their energies.

- $t\bar{t}H$: We integrate over the energy of one of the b quarks from the Higgs decay. The other quark’s energy is fixed by the requirement that their invariant mass be equal to the Higgs mass (NWA). In MoMEMta, this is achieved by applying the transformation of the “Secondary Block C/D”, and fixing s_{12} to m_H .

Using the above parameterisation, the peaks in the integrand remain mapped to the integration variables, and the unobserved degrees of freedom due to the two neutrinos in the final state are effectively removed. Finally, the integrand needs to be averaged over every one of the $4! = 24$ possible assignments between jets and partons. By using an additional integration variable controlling which assignment should be considered, the weights are obtained from a single call to the integration routine, and adaptive integration algorithms automatically focus on those assignments yielding large contribution to the final answer.

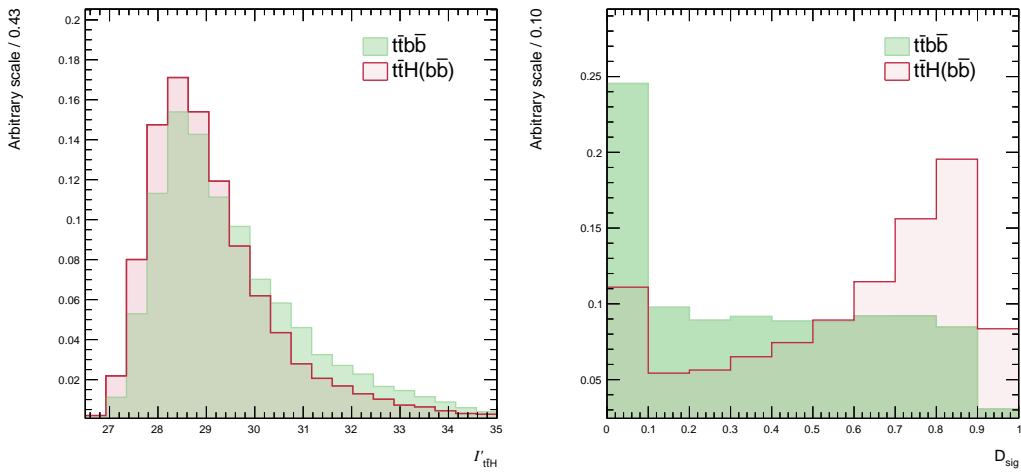


Figure 3. Left: signal information under the signal hypothesis ($t\bar{t}H$). Right: discriminating variable built from the weights in the signal and background hypotheses. All distributions are normalised to unity.

Figure 3 shows the normalised distributions of the event information $I'_{t\bar{t}H}$ and a discriminating variable defined as

$$\mathcal{D}_{\text{sig}}(x) = \left(1 + \frac{P(x|t\bar{t}b\bar{b})}{P(x|t\bar{t}H)} \right)^{-1}. \quad (4.4)$$

By applying a requirement on \mathcal{D}_{sig} such that 50% of the $t\bar{t}H$ signal is retained, 83% of the $t\bar{t} + \text{jets}$ background can be rejected. As a comparison, using the invariant masses of b -tagged jets in the events would only reject 65% of the background for the same signal efficiency.

5 Indicative performance figures

We give approximate performance figures observed when computing weights for the different use-cases presented above. It should be clear that those number are indicative only, as the computation time strongly depends on the considered hypothesis and the parameters of the numerical integration

algorithm. Furthermore, these results were obtained using the functionalities available out-of-the-box in MoMEMta, and with matrix elements generated by our plugin for MG5_AMC@NLO, which means no attempt whatsoever was made towards optimising the computation for these particular cases. MoMEMta has been designed with the aim of being flexible, enabling users to implement simplifications or optimisations fit for their needs. Note that tuning the parameters of the algorithms used for the numerical integration of the weights can have a strong impact on both the precision p of the resulting integrals (which in turns impacts the power of the discriminant built from the weights), and the overall computation time T . Generally, all other things being equal, the evaluation time T scales roughly as $T \propto p^{-2}$. The computation of the weights used in Sec. 4.3 was carried out using two different integration algorithms available in the CUBA library: Vegas and Divonne. The latter was found to yield substantially shorter completion times, without compromising the discrimination between signal and background with respect to the former.

In Tab. 3 we give the average per-event computation times for the weights used in the examples of Sec. 4, along with the average relative precision on these weights reported by the integration algorithm. These results were obtained on a computer cluster with an average per-core HS06 score¹ of 9.1. Table 4 shows how much time is spent on the main elements of the computation. These fractions are indicative and vary from event to event, but show that for complex hypotheses such as those considered in Sec. 4.3, the bottleneck in the computation is due to the evaluation of the matrix element.

The memory consumption of MoMEMta is strongly linked to the way the integration algorithm is configured. In practice, for the examples shown here, memory consumption was observed never to exceed 200 MB.

Table 3. Average computation time of weights under the different hypotheses used in Sec. 4. The average relative precision on the resulting weights are also given.

Hypothesis	Avg. time	Avg. precision
$gg \rightarrow H \rightarrow ZZ^* \rightarrow 4l, q\bar{q} \rightarrow ZZ^*/\gamma^* \rightarrow 4l$	0.6 ms	/
$tW^-, \bar{t}W^+$	4.5 s	2.3%
$t\bar{t}H(b\bar{b})$ (Vegas)	140 s	0.9%
$t\bar{t}b\bar{b}$ (Vegas)	700 s	1.0%
$t\bar{t}H(b\bar{b})$ (Divonne)	90 s	0.5%
$t\bar{t}b\bar{b}$ (Divonne)	600 s	0.6%

6 Summary

We have presented MoMEMta, a modular software package to compute the convolution integrals at the core of the MEM. Its modular structure covers the needs of experimental analysis workflows at the LHC without compromising the ease of use on simpler and smaller simulated samples used for phenomenological studies.

¹<https://w3.hepik.org/benchmarking.html>

Table 4. Indicative shares of computation time due to the different elements entering the evaluation of weights under different hypotheses. The elements shown are the evaluation of the matrix element, the parton distribution functions and the transfer functions, the generation of the phase-space (including the change of variables introduced in Sec. 3), and the various remaining tasks.

Hypothesis	Matrix element	PDF	Transfer functions	Phase-space	Various
$t\bar{W}^-, \bar{t}W^+$	22%	11%	23%	22%	22%
$t\bar{t}H(b\bar{b})$	93%	1.0%	2.4%	2.3%	1.4%
$t\bar{t}b\bar{b}$	98%	0.5%	0.5%	0.4%	0.3%

The MEM is used in HEP by both theoretical and experimental communities with different purposes and levels of complexity ranging from the evaluation of a matrix element on a reconstructed event to the precise evaluation of model parameters through the use of the properly normalised likelihood. We have described a few use cases of the MEM for signal extraction in LHC analyses showcasing the different levels of complexity. From the most simple implementation, for Higgs boson characterisation in the $H \rightarrow ZZ^* \rightarrow 4l$ channel, to a complex final states such as $t\bar{t}H$ production, MoMEMta has proven to be as performing as previous implementations.

MoMEMta is designed to offer a flexible and reusable framework for a wide range of applications of the MEM. It aims at implementing a wide range of possibilities while letting the user in control of the subset of features actually used for a particular application. It also allows the user to substitute optimised code for part of the integration while profiting from other facilities. A typical example would be the use of an optimised matrix element implementation while keeping the benefits of the I/O, configuration, and integration framework.

The modular structure of MoMEMta lets us envisage a rich set of future developments. To cite a few, we consider adding an interface to matrix element libraries such as MCFM [24] or Sherpa [55], extending the integration over missing (unreconstructed) objects or on the contrary on additional objects present in the reconstructed event, or extending the transfer function to include an efficiency term. Other developments could further enhance the performance of the integration itself, through the use of vector integrand with modified transfer function to evaluate the effect of systematic uncertainties, or through the use of machine-learning inspired integration algorithms [56].

7 Acknowledgments

We warmly thank Andrea Giammanco and Olivier Mattelaer for their valued feedback. This project is funded by FRS-FNRS (Belgian National Scientific Research Fund) IISN projects 4.4503.17 and 4.4503.16. MoMEMta is part of AMVA4NP, a project that has received funding from the European Horizon 2020 research and innovation programme under grant agreement N^o675440. SW is supported through a FRIA grant by the FRS-FNRS. Computational resources have been provided by the supercomputing facilities of the Université catholique de Louvain (CISM/UCL) and the Consortium des Équipements de Calcul Intensif en Fédération Wallonie Bruxelles (CÉCI) funded by the Fond de la Recherche Scientifique de Belgique (F.R.S.-FNRS) under convention 2.5020.11. This work would not have been possible without the help of the MADWEIGHT team. Special thanks to Matthias Komm who designed our logo.

References

- [1] G. Aad *et al.* [ATLAS Collaboration], “Observation of a new particle in the search for the Standard Model Higgs boson with the ATLAS detector at the LHC,” *Phys. Lett. B* **716** (2012) 1 doi:10.1016/j.physletb.2012.08.020 [arXiv:1207.7214 [hep-ex]]
- [2] S. Chatrchyan *et al.* [CMS Collaboration], “Observation of a new boson at a mass of 125 GeV with the CMS experiment at the LHC,” *Phys. Lett. B* **716** (2012) 30 doi:10.1016/j.physletb.2012.08.021 [arXiv:1207.7235 [hep-ex]]
- [3] K. Kondo, “Dynamical Likelihood Method for Reconstruction of Events with Missing Momentum. I. Method and Toy Models,” *J. Phys. Soc. Jpn.* **57** (1988) 4126–4140 doi:10.1143/JPSJ.57.4126
- [4] K. Kondo, “Dynamical Likelihood Method for Reconstruction of Events with Missing Momentum. II. Mass Spectra for $2 \rightarrow 2$ Processes,” *J. Phys. Soc. Jpn.* **60** (1991) 836–844 doi:10.1143/JPSJ.60.836
- [5] S. Abachi *et al.* [D0 Collaboration], “Search for the top quark in $p\bar{p}$ collisions at $\sqrt{s} = 1.8$ TeV,” *Phys. Rev. Lett.* **72** (1994) 2138. doi:10.1103/PhysRevLett.72.2138
- [6] V. M. Abazov *et al.* [D0 Collaboration], “A precision measurement of the mass of the top quark,” *Nature* **429** (2004) 638 doi:10.1038/nature02589 [arXiv:0406031 [hep-ex]]
- [7] V. M. Abazov *et al.* [D0 Collaboration], “Measurement of the top quark mass in the lepton+jets final state with the matrix element method,” *Phys. Rev. D* **74** (2006) 092005 doi:10.1103/PhysRevD.74.092005 [arXiv:0609053 [hep-ex]]
- [8] A. Abulencia *et al.* [CDF Collaboration], “Precise measurement of the top quark mass in the lepton+jets topology at CDF II,” *Phys. Rev. Lett.* **99** (2007) 182002 doi:10.1103/PhysRevLett.99.182002 [arXiv:0703045 [hep-ex]]
- [9] A. Abulencia *et al.* [CDF Collaboration], “Precision measurement of the top quark mass from dilepton events at CDF II,” *Phys. Rev. D* **75** (2007) 031105 doi:10.1103/PhysRevD.75.031105 [arXiv:0612060 [hep-ex]]
- [10] V. M. Abazov *et al.* [D0 Collaboration], “Measurement of the top quark mass in the dilepton channel,” *Phys. Lett. B* **655** (2007) 7 doi:10.1016/j.physletb.2007.08.074 [arXiv:0609056 [hep-ex]]
- [11] G. Aad *et al.* [ATLAS Collaboration], “Search for the Standard Model Higgs boson produced in association with top quarks and decaying into $b\bar{b}$ in pp collisions at $\sqrt{s} = 8$ TeV with the ATLAS detector,” *Eur. Phys. J. C* **75** (2015) no. 7, 349 doi:10.1140/epjc/s10052-015-3543-1 [arXiv:1503.05066 [hep-ex]]
- [12] M. Aaboud *et al.* [ATLAS Collaboration], “Search for the Standard Model Higgs boson produced in association with top quarks and decaying into a $b\bar{b}$ pair in pp collisions at $\sqrt{s} = 13$ TeV with the ATLAS detector,” Submitted to *Phys. Rev. D* [arXiv:1712.08895 [hep-ex]]
- [13] V. Khachatryan *et al.* [CMS Collaboration], “Search for a Standard Model Higgs Boson Produced in Association with a Top-Quark Pair and Decaying to Bottom Quarks Using a Matrix Element Method,” *Eur. Phys. J. C* **75** (2015) no.6, 251 doi:10.1140/epjc/s10052-015-3454-1 [arXiv:1502.02485 [hep-ex]]
- [14] A. M. Sirunyan *et al.* [CMS Collaboration], “Search for $t\bar{t}H$ production in the $H \rightarrow b\bar{b}$ decay channel with leptonic $t\bar{t}$ decays in proton-proton collisions at $\sqrt{s} = 13$ TeV,” Submitted to *JHEP*. [arXiv:1804.03682 [hep-ex]]
- [15] A. M. Sirunyan *et al.* [CMS Collaboration], “Search for $t\bar{t}H$ production in the all-jet final state in proton-proton collisions at $\sqrt{s} = 13$ TeV,” Submitted to *JHEP*. [arXiv:1803.06986 [hep-ex]]

- [16] M. Aaboud *et al.* [ATLAS Collaboration], “Measurement of the Higgs boson coupling properties in the $H \rightarrow ZZ^* \rightarrow 4\ell$ decay channel at $\sqrt{s} = 13$ TeV with the ATLAS detector,” Submitted to JHEP [arXiv:1712.02304 [hep-ex]]
- [17] M. Aaboud *et al.* [ATLAS Collaboration], “Evidence for the associated production of the Higgs boson and a top quark pair with the ATLAS detector,” Phys. Rev. D **97** (2018) no.7, 072003 doi:10.1103/PhysRevD.97.072003 [arXiv:1712.08891 [hep-ex]].
- [18] A. M. Sirunyan *et al.* [CMS Collaboration], “Evidence for associated production of a Higgs boson with a top quark pair in final states with electrons, muons, and hadronically decaying τ leptons at $\sqrt{s} = 13$ TeV,” Submitted to JHEP. [arXiv:1803.05485 [hep-ex]]
- [19] G. Aad *et al.* [ATLAS Collaboration], “Evidence for single top-quark production in the s -channel in proton-proton collisions at $\sqrt{s} = 8$ TeV with the ATLAS detector using the Matrix Element Method,” Phys. Lett. B **756** (2016) 228–246 doi:10.1016/j.physletb.2016.03.017 [arXiv:1511.05980 [hep-ex]]
- [20] V. Khachatryan *et al.* [CMS Collaboration], “Measurement of spin correlations in $t\bar{t}$ production using the matrix element method in the muon+jets final state in pp collisions at $\sqrt{s} = 8$ TeV,” Phys. Lett. B **758** (2016) 321 doi:10.1016/j.physletb.2016.05.005 [arXiv:1511.06170 [hep-ex]].
- [21] P. Artoisenet, V. Lemaitre, F. Maltoni and O. Mattelaer, “Automation of the matrix element reweighting method,” JHEP **1012** (2010) 068 doi:10.1007/JHEP12(2010)068 [arXiv:1007.3300 [hep-ph]]
- [22] F. Fiedler, A. Grohsjean, P. Haefner and P. Schieferdecker, “The Matrix Element Method and its Application in Measurements of the Top Quark Mass,” Nucl. Instrum. Meth. A **624** (2010) 203 doi:10.1016/j.nima.2010.09.024 [arXiv:1003.1316 [hep-ex]]
- [23] J. Alwall *et al.*, “The automated computation of tree-level and next-to-leading order differential cross sections, and their matching to parton shower simulations,” JHEP **1407** (2014) 079 doi:10.1007/JHEP07(2014)079 [arXiv:1405.0301 [hep-ph]]
- [24] J. M. Campbell, R. K. Ellis and W. T. Giele, “A Multi-Threaded Version of MCFM,” Eur. Phys. J. C **75** (2015) no.6, 246 doi:10.1140/epjc/s10052-015-3461-2 [arXiv:1503.06182 [physics.comp-ph]]
- [25] D. E. Ferreira de Lima, O. Mattelaer and M. Spannowsky, “Reconstructing the invisible with matrix elements,” [arXiv:1712.03266 [hep-ph]]
- [26] J. Neyman, E. S. Pearson, “On the problem of the most efficient tests of statistical hypotheses,” Phil. Trans. R. Soc. Lond. A (1933) 231 289–337 doi: 10.1098/rsta.1933.0009
- [27] R. Ierusalimsky, L. Henrique de Figueiredo, and W. Celes Filho, “Lua — an extensible extension language,” Software: Practice & Experience **26** no. 6 (1996) 635–652 doi:10.1002/(SICI)1097-024X(199606)26:6<635::AID-SPE26>3.0.CO;2-P
- [28] Rene Brun and Fons Rademakers, “ROOT - An Object Oriented Data Analysis Framework”, Proceedings AIHENP’96 Workshop, Lausanne, Sep. 1996, Nucl. Inst. & Meth. in Phys. Res. A 389 (1997) 81-86. See also <http://root.cern.ch/>
- [29] M. Dobbs and J. B. Hansen, “The HepMC C++ Monte Carlo event record for High Energy”, Physics Comput. Phys. Commun. 134, 41 (2001).
- [30] J. Thaler, “How to Read LHC Olympics Data Files”, <http://madgraph.phys.ucl.ac.be/Manual/lhco.html> (2006), Accessed: February 2018.
- [31] L. Garren, P. Lebrun, “StdHep User Manual”, <http://cepa.fnal.gov/psm/stdhep/>, Accessed: February 2018.

- [32] Sébastien Brochet, Sébastien Wertz, Jérôme de Favereau “MoMEMta - MadGraph Matrix Element Exporter”, May 2018, doi:10.5281/zenodo.1250685
- [33] A. Buckley, J. Ferrando, S. Lloyd, K. Nordström, B. Page, M. Rätzjenacht, M. Schönherr and G. Watt, “LHAPDF6: parton density access in the LHC precision era,” *Eur. Phys. J. C* **75** (2015) 132 doi:10.1140/epjc/s10052-015-3318-8 [arXiv:1412.7420 [hep-ph]]
- [34] T. Hahn, “CUBA: A Library for multidimensional numerical integration,” *Comput. Phys. Commun.* **168** (2005) 78 doi:10.1016/j.cpc.2005.01.010 [arXiv:0404043 [hep-ph]]
- [35] G.P. Lepage, “A New Algorithm for Adaptive Multidimensional Integration,” *J. Comput. Phys.* **27** (1978) 192 doi:10.1016/0021-9991(78)90004-9
- [36] J.H. Friedman, M.H. Wright, “A Nested Partitioning Procedure for Numerical Multiple Integration and Adaptive Importance Sampling,” *ACM Trans. Math. Software* **7** (1981) 76 doi:10.1145/355934.355939
- [37] J. Berntsen, T.O. Espelid and A. Genz, “An adaptive algorithm for the approximate calculation of multiple integrals,” *ACM Trans. Math. Software* **17** (1991) 437–451 doi:10.1145/210232.210233
- [38] J. Berntsen, T.O. Espelid and A. Genz, “Algorithm 698: DCUHRE: an adaptive multidimensional integration routine for a vector of integrals,” *ACM Trans. Math. Software* **17** (1991) 452–456 doi:10.1145/210232.210234
- [39] Sébastien Brochet, Sébastien Wertz, Miguel Vidal, Brieuc François, Alessia Saggio, Christophe Delaere, and Vincent Lemaître, “Momenta/momenta: 1.0.0”, May 2018, doi:10.5281/zenodo.1250697
- [40] Sébastien Brochet, Sébastien Wertz, Miguel Vidal, Brieuc François, Alessia Saggio, Christophe Delaere, and Vincent Lemaître, “The MoMEMta project website”, May 2018, doi:10.5281/zenodo.1250743
- [41] Sébastien Brochet, Sébastien Wertz, Alessia Saggio “MoMEMta/Tutorials (Version v1.0.0)”, May 2018, doi:10.5281/zenodo.1250682
- [42] T. Sjöstrand *et al.*, “An Introduction to PYTHIA 8.2,” *Comput. Phys. Commun.* **191** (2015) 159 doi:10.1016/j.cpc.2015.01.024 [arXiv:1410.3012 [hep-ph]]
- [43] J. de Favereau *et al.*, “DELPHES 3, A modular framework for fast simulation of a generic collider experiment,” *JHEP* **1402** (2014) 057 doi:10.1007/JHEP02(2014)057 [arXiv:1307.6346 [hep-ex]]
- [44] G. Aad *et al.* [ATLAS Collaboration], “Measurements of Higgs boson production and couplings in the four-lepton channel in pp collisions at center-of-mass energies of 7 and 8 TeV with the ATLAS detector,” *Phys. Rev. D* **91** (2015) no. 1, 012006 doi:10.1103/PhysRevD.91.012006 [arXiv:1408.5191 [hep-ex]]
- [45] G. Aad *et al.* [ATLAS Collaboration], “Study of the spin and parity of the Higgs boson in diboson decays with the ATLAS detector,” *Eur. Phys. J. C* **75** (2015) no. 10, 476 Erratum: [*Eur. Phys. J. C* **76** (2016) no. 3, 152] doi:10.1140/epjc/s10052-015-3685-1, 10.1140/epjc/s10052-016-3934-y [arXiv:1506.05669 [hep-ex]]
- [46] A. M. Sirunyan *et al.* [CMS Collaboration], “Measurements of properties of the Higgs boson decaying into the four-lepton final state in pp collisions at $\sqrt{s} = 13$ TeV,” *JHEP* **1711** (2017) 047 doi:10.1007/JHEP11(2017)047 [arXiv:1706.09936 [hep-ex]]
- [47] A. M. Sirunyan *et al.* [CMS Collaboration], “Constraints on anomalous Higgs boson couplings using production and decay information in the four-lepton final state,” *Phys. Lett. B* **775** (2017) 1 doi:10.1016/j.physletb.2017.10.021 [arXiv:1707.00541 [hep-ex]]

- [48] S. Bolognesi, Y. Gao, A. V. Gritsan, K. Melnikov, M. Schulze, N. V. Tran and A. Whitbeck, “On the spin and parity of a single-produced resonance at the LHC,” *Phys. Rev. D* **86** (2012) 095031 doi:10.1103/PhysRevD.86.095031 [arXiv:1208.4018 [hep-ph]]
- [49] I. Anderson *et al.*, “Constraining anomalous HVV interactions at proton and lepton colliders,” *Phys. Rev. D* **89** (2014) no. 3, 035007 doi:10.1103/PhysRevD.89.035007 [arXiv:1309.4819 [hep-ph]]
- [50] P. Artoisenet *et al.*, “A framework for Higgs characterisation,” *JHEP* **1311** (2013) 043 doi:10.1007/JHEP11(2013)043 [arXiv:1306.6464 [hep-ph]]
- [51] T. Aaltonen *et al.* [CDF Collaboration], “First Observation of Electroweak Single Top Quark Production,” *Phys. Rev. Lett.* **103** (2009) 092002 doi:10.1103/PhysRevLett.103.092002 [arXiv:0903.0885 [hep-ex]]
- [52] V. M. Abazov *et al.* [D0 Collaboration], “Observation of Single Top Quark Production,” *Phys. Rev. Lett.* **103** (2009) 092001 doi:10.1103/PhysRevLett.103.092001 [arXiv:0903.0850 [hep-ex]]
- [53] E. Alvarez, L. Da Rold, M. Estevez and J. F. Kamenik, “Measuring $|V_{td}|$ at the LHC,” *Phys. Rev. D* **97** (2018) no.3, 033002 doi:10.1103/PhysRevD.97.033002 [arXiv:1709.07887 [hep-ph]]
- [54] P. Artoisenet, P. de Aquino, F. Maltoni and O. Mattelaer, “Unravelling $t\bar{t}h$ via the Matrix Element Method,” *Phys. Rev. Lett.* **111** (2013) no.9, 091802 doi:10.1103/PhysRevLett.111.091802 [arXiv:1304.6414 [hep-ph]].
- [55] T. Gleisberg, S. Hoeche, F. Krauss, M. Schonherr, S. Schumann, F. Siegert and J. Winter, “Event generation with SHERPA 1.1,” *JHEP* **0902** (2009) 007 doi:10.1088/1126-6708/2009/02/007 [arXiv:0811.4622 [hep-ph]]
- [56] J. Bendavid, “Efficient Monte Carlo Integration Using Boosted Decision Trees and Generative Deep Neural Networks,” [arXiv:1707.00028 [hep-ph]]